Revista Brasileira de Geofísica
RBGf
Brazilian Journal of Geophysics

Revista Brasileira de Geofísica (2014) 32(4): 615-636

ISSN 0102-261X
www.scielo.br/rbg

METEOROLOGICAL TIDES AND EPISODES OF SEVERE COASTAL EROSION ON THE COAST OF SALVADOR, BAHIA STATE, BRAZIL

Flavia R.L.S. Dutra[1], Mauro Cirano[2,3], Abilio C.S.P. Bittencourt[4], Clemente A.S. Tanajura[2,3] and Mateus Lima[3]

ABSTRACT. The coastline of Bahia State, Brazil, in the eastern sector of the northeastern region of Brazil, has a total of 20 beaches, 14 of which are located on the open sea (Atlantic Ocean), while the others are sheltered in the Todos os Santos Bay. Many of these beaches have been or are currently being affected by episodes of severe coastal erosion which are intrinsically related to both anthropogenic and natural processes. This study aimed to use statistical analyses of information and data, such as photos, texts from local newspapers, synoptic maps and reanalysis data from the National Centers for Environmental Prediction to identify severe erosion events related to meteorological tides on the Salvador coastline during the period from 1965 to 2006. The results show that most erosion events appear to be associated with the occurrence of meteorological tides and have great destructive potential. We found that the combination of i) the occurrence of spring tides with ii) the arrival of cold fronts and/or coupling of a high pressure system with a trough in the lower levels of the atmosphere and iii) winds predominately from S and SE, that through Ekman transport, promotes pilling up of water against the coast, favours the increase of the water level and wave height and range along the coast.

Keywords: cold fronts, Ekman transport, spring-tides, severe coastal erosion.

RESUMO. O litoral de Salvador, no Estado da Bahia, possui um total de 20 praias, das quais 14 estão localizadas em região de mar aberto, no setor leste do Nordeste brasileiro, banhadas pelo oceano Atlântico, enquanto que as demais se encontram abrigadas na Baía de Todos os Santos. Dentre estas praias, muitas foram ou estão sendo acometidas por episódios de erosão costeira severa, que estão intrinsecamente relacionados à ação tanto de origem antrópica quanto natural. O presente estudo visou, através de análises e estatísticas de informações e dados como fotos, textos de jornais locais e cartas sinóticas e reanálises do National Centers for Environmental Prediction dos EUA, identificar os eventos de erosão severa relacionados à ocorrência de marés meteorológicas na orla de Salvador, no período de 1965 a 2006. Os resultados mostram que a maior parte dos eventos erosivos parece estar associada à ocorrência de marés meteorológicas, com grande potencial destrutivo. Este estudo permitiu constatar que a combinação: i) da ocorrência de marés de sizígia, com ii) a chegada de frentes frias e/ou o acoplamento de uma alta pressão a um cavado, nos baixos níveis da atmosfera, e iii) a predominância de ventos de S e SE, que através do transporte de Ekman, promovem empilhamento de água contra a costa, cria uma conjunção que favorece a sobre-elevação da altura e do alcance das ondas ao longo da costa.

Palavras-chave: frentes frias, transporte de Ekman, maré de sizígia, erosão costeira severa.

[1]Universidade Federal de Minas Gerais, Programa de Pós-Graduação em Geografia Física, Instituto de Geociências, Campus Pampulha, Belo Horizonte, MG, Brazil – E-mail: frlacerda@yahoo.com.br

[2]Universidade Federal da Bahia, Departamento de Física da Terra e do Meio Ambiente (DFTMA), Instituto de Física, Campus Ondina, 40170-280 Salvador, BA, Brazil – E-mails: mcirano@ufba.br; cast@ufba.br

[3]Universidade Federal da Bahia, Grupo de Oceanografia Tropical (GOAT), Instituto de Física, Campus Ondina, 40170-280 Salvador, BA, Brazil – E-mail: matdolima@gmail.com

[4]Universidade Federal da Bahia, Instituto de Geociências, Laboratório de Estudos Costeiros (LEC), Centro de Pesquisa em Geofísica e Geologia (CPGG), Campus Ondina, 40170-280 Salvador, BA, Brazil – E-mail: abilio@pq.cnpq.br

INTRODUCTION

Coastal areas are, by definition, the interface between the land and ocean, and their physical characteristics and dynamics are constantly changing. Approximately one quarter of the Brazilian population now lives in coastal regions, where the continuous action of the sea causes the erosion, transport and deposition of sediment, thereby resulting in the constant shifting of the coastline. In addition to these processes, the impact of human activities in coastal areas is very high and often overlaps with the action of natural forces to exacerbate their effects, for example, by worsening the effects of erosion along the coast (e.g., Dominguez & Bittencourt, 1996; Komar, 1998; Haslett, 2000; Pivel et al., 2002; Tessler & Goya, 2005). Among the possible human impacts that can occur along shorelines, several authors (e.g., Neves & Muehe, 1995; Komar, 1998; Neves, 2003) have noted the presence of coastal protection infrastructure such as retaining walls, breakwaters and jetties, among others. These stabilization structures are very common along modern-day beaches but are often very rigid and/or inadequate for their intended function. They affect the sediment budget and can result in an excess or deficiency of sediment supply along the coast.

Coastal erosion and flooding along low-sloping oceanic coasts are mainly generated by storms that cause increased sea levels compared to regular tides (Parise et al., 2009). Meteorological tides, which are basically defined as the difference between predicted and observed tides, are one of the major natural risks faced by coastal communities and are the main cause of loss of property, lives and natural habitats (Murty, 1988).

The coastal region of Salvador is highly urbanized, with public or private development that includes seaside houses, walkways and plazas. Often, these structures are located in areas under imminent risk of erosion due their proximity to the high-water line of spring tides. As a result, economic losses often occur from erosion in this sector of the state of Bahia.

In one study of coastal erosion in northeastern Brazil, Dominguez & Bittencourt (1996) concluded that coastal erosion in the region was intrinsically related to the sediment budget, without any relation to sea level rise, as suggested by Neves & Muehe (1995). In a study of Salvador's Atlantic coast, Bittencourt et al. (2000, 2005) identified a littoral cell characterized by net longshore drift with a NE-SW direction. This cell has increased potential drift intensity in the downdrift direction; therefore, there is a deficit in long-term sediment accumulation along that coastal stretch. According to Medeiros (2005) and Bittencourt et al. (2008), there is a correlation between severe coastal erosion events in Salvador and storm surges characterized by strong winds and large waves, which are associated with the periodic arrival of cold fronts.

This study aimed to evaluate the role of atmospheric and oceanographic processes as drivers of severe coastal erosion events on the coast of Salvador during the period 1965-2006 to provide information for improving urban planning in Salvador.

STUDY AREA

The city of Salvador, centered at a latitude of 12°58′S and a longitude of 38°39′W, is located on the eastern coast of northeastern Brazil (NEB) (Fig. 1). The eastern sector of the city is bordered by the Atlantic Ocean and the western sector by the Todos os Santos Bay (hereafter TSB). Severe erosion occurs along the Salvador coastline from the beaches of Roma (Number 1 in Fig. 1) to Itapuã (Number 14 in Fig. 1). These events occur on sandy beaches with intermediate to reflective morphodynamics.

As shown in Figure 1, the Salvador coastline has a narrow continental shelf (approximately width of 10 km) with a shelf-break occurring at approximately 50 m in depth. A significant bottom topographic feature can be observed in front of the Barra beach (beach Number 6), which consists of a shallow sandy bank approximately 5 km long.

With respect to coastal circulation in the region, Cirano & Lessa (2007) found that circulation outside the TSB undergoes seasonal variation with two distinct patterns: a predominantly southwestward circulation during the dry season (summer) and a predominantly northeastward circulation during the rainy season (autumn-winter). These authors also found that the TSB is more protected during the summer, mainly due to the presence of easterly winds. Also, internal oscillations within the bay are subject to a relatively low degree of interference from prevailing oceanographic conditions on the continental shelf. In contrast, on the continental shelf, there is a strong coupling between oscillations and circulation, particularly during the autumn-winter season. This interaction mainly occurs due to an increased frequency of cold fronts in the region during this season, which cause SE winds to blow over the coast and the TSB, altering prevailing circulation patterns.

The climate on the east coast of the NEB is hot and humid, with the highest total rainfall concentrated between March and July (autumn-winter) and rainfall maxima occurring in April and May (INMET, 2010). This pattern varies spatially and temporally depending on precipitation dynamics related to atmospheric circulation systems at various scales, including easterly wave disturbances, sea-breeze-induced instability lines, the South Atlantic subtropical anticyclone, frontal systems (Kousky & Chu, 1978;

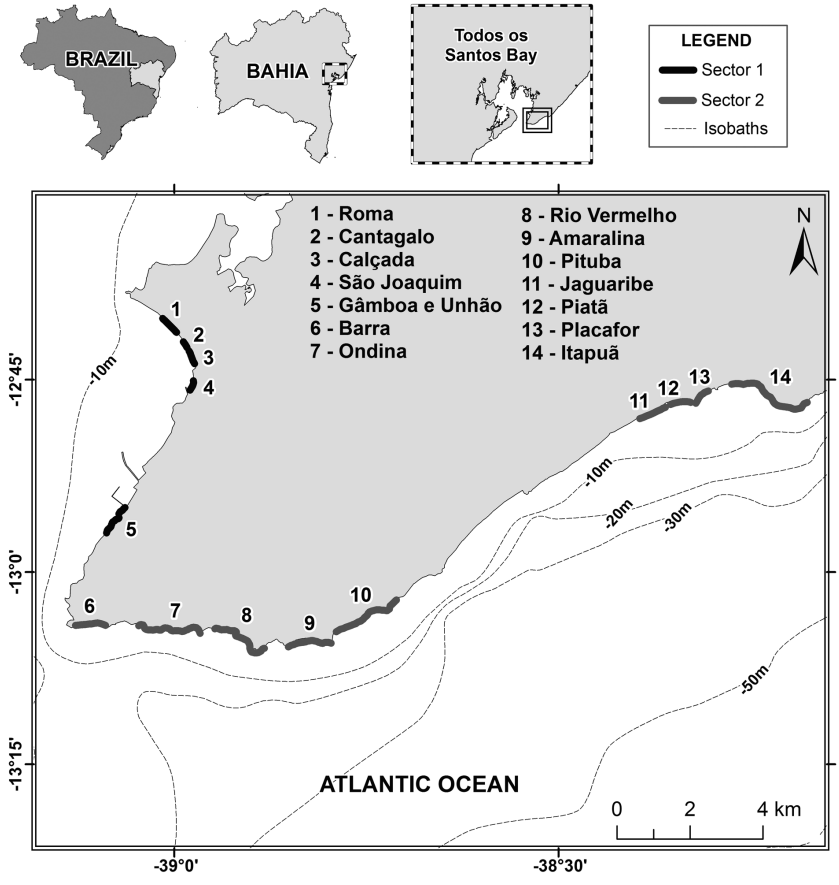

Figure 1 – Salvador coastline map, where the numbers 1 to 14 indicate the beaches that there were historic registers of severe coastal erosion events.

Kousky, 1980; Lima, 1991) and interannual variability associated with the sea surface temperature (SST) of the Atlantic Ocean and the El Niño/Southern Oscillation (ENSO) phenomenon (e.g., Wang, 2002; Grimm, 2003; Wang et al., 2010).

METHODOLOGY

In this study, a conceptual model for characterizing erosion events from 1965-2006 and case studies using the model were performed using the following data sources:

i) Sites of severe coastal erosion events obtained from local newspapers ("A Tarde", "Estado da Bahia" and "Correio da Bahia") along the Salvador coastline, including the region sheltered by the TSB, for the period from 1965-2006;

ii) Daily synoptic charts and predicted maximum tide heights for the port of Salvador, provided by the Directorate of Hydrography and Navigation of the Brazilian Navy (Diretoria de Hidrografia e Navegação – DHN). Only data for the erosion events were obtained;

iii) Wave refraction diagrams for southeasterly waves along the coastal stretch corresponding to the Atlantic coast of Salvador (Bittencourt et al., 2008);

iv) Monthly data for the central equatorial Pacific SST for the entire study period and monthly climatology data for mean sea level pressure (MSLP) for the period 1968-1996, both obtained from the Center for Weather Forecasting and Climate Studies/National Institute for Space Research (Centro de Previsão de Tempo e Estudos Climáticos/ Instituto Nacional de Pesquisas Espaciais – CPTEC/INPE);

v) Daily zonal (u) and meridional (v) wind components at 10 m and MSLP at 00, 06, 12 and 18 UTC on a 2.5° × 2.5° grid, obtained from reanalysis by the National Centers for Environmental Prediction (NCEP) for the period 1965-2006;

vi) Historical series of precipitation data from 1965 until 2006 and monthly data for average wind speed from 1975 until 1998, both collected at the Ondina weather station in

Salvador by the Brazilian National Institute of Meteorology (Instituto Nacional de Meteorologia – INMET); and

vii) Daily results of significant wave height and wave period at 00, 06, 12 and 18 UTC in the oceanic region off the coast of Salvador for the period of erosion events described in the case studies, obtained from reanalysis project ERA-40.

To characterize wave patterns and generate a wave refraction diagram, wave data from visual observations at high sea were used (Hogben & Lumb, 1967).

The conceptual model used in this study aimed to demonstrate and qualitatively explain the main forces involved in the process of coastal erosion along the Salvador shoreline, which is associated with the occurrence of meteorological tides. The main driving forces were described in descending order of importance of each parameter, mainly based on the results of statistical analyses, which were used to validate the model.

To characterize the context in which coastal erosion events occurred over the study period, all erosion events were defined by their erosion period (EP), which was subdivided into three periods: two days before erosion (BE), erosion day (ED) and one day after erosion. The following analyses were subsequently performed.

i) Statistical parameters were calculated for the u and v wind components and MSLP: mean variation across the area bounded by the coordinates 12.5° S and 14° S/37.0° W and 39.5° W and distribution and standard deviation of these fields;

ii) Predicted maximum tide height and the type of tide on ED were determined and total rainfall recorded in Salvador was determined for the EP;

iii) Four synoptic scenarios were identified based on the above information, and an analysis of surface synoptic maps was performed for each erosion event;

iv) A case study of an erosion event was completed for each scenario, by determining the predicted maximum tide height on ED, resulting in a total of four events.

Observation of the surface synoptic maps was used to describe circulation patterns by identifying the synoptic systems that were active at the time of the events. Two main synoptic scenarios were identified that favored the occurrence of erosion along the Salvador shoreline. These scenarios were each subdivided into two additional scenarios due to small but significant differences in synoptic features, mainly based on the behavior of the meridional wind component and its influence on erosion intensity.

Finally, case studies were used for a detailed evaluation of daily temporal and spatial evolution in the synoptic systems during the EP, with the purpose of developing a conceptual understanding of how local coastal circulation dynamics along the Salvador shoreline developed during erosion events. For this purpose, fields of meteorological variables from the ERA-40 reanalysis, tidal predictions for the port of Salvador, rainfall data, information about tide type, wave data and surface synoptic maps were used. The purpose of the study was to better understand the spatial and temporal evolution of active weather systems during coastal erosion events along the Salvador shoreline, about which there is generally a lack of detailed knowledge.

RESULTS AND DISCUSSION

In total, 31 erosion events during the period from 1965 to 2006 were identified. This number represents an increase of 14 erosion events over a 28-year timeframe, when compared with 17 erosion events identified by Medeiros (2005) and Bittencourt et al. (2008) for a 13 year data series from 1990-2003. The events in this study occurred on beaches in Sector 1 (beaches sheltered by TSB) and 2 (beaches in the region of open sea, bordered by the Atlantic Ocean) (Fig. 1). The initial identification of coastal erosion events was based on evidence of material damage along the Salvador coastline obtained from narratives and/or photos from local newspapers, which allowed determination of the location of affected beaches and neighborhoods, dating of the event and characterization of the type of destruction. Subsequently, a conceptual model was created that facilitated the classification of the most severe erosion events, which will be discussed in the first part of this section. In the second part of this section, case studies for two of the main types of scenarios identified are discussed.

The monthly frequency of severe coastal erosion events along the Salvador shoreline is shown in Figure 2. This graph shows that most events occurred during the months of March and August, with six events per month, followed by the months of May, July and September, with five events per month. The highest frequency occurred in the autumn and winter seasons, showing a strong seasonal signal. The greater occurrence of coastal erosion during these seasons is consistent with the findings of Kousky (1979) and Andrade (2005), who demonstrated that frontal systems along the Bahia coast had a greater influence during autumn and winter. The months of April and June showed the lowest erosion event frequencies, with three and one event per month, respectively.

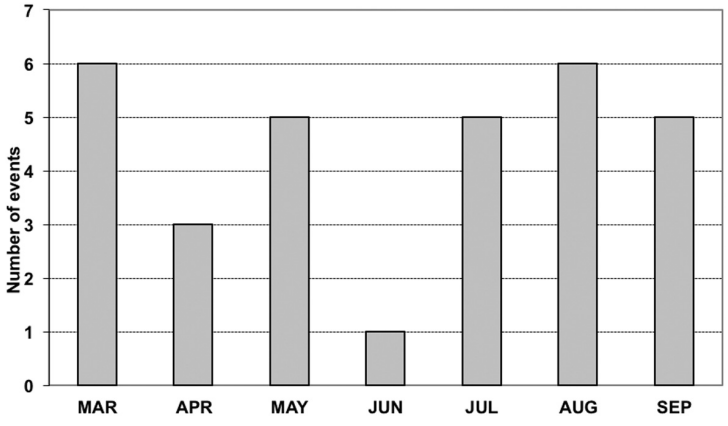

Figure 2 – Monthly frequencies of coastal erosion with damage on the Salvador coastline during the period from 1965 to 2006 (Source: *A Tarde* newspaper).

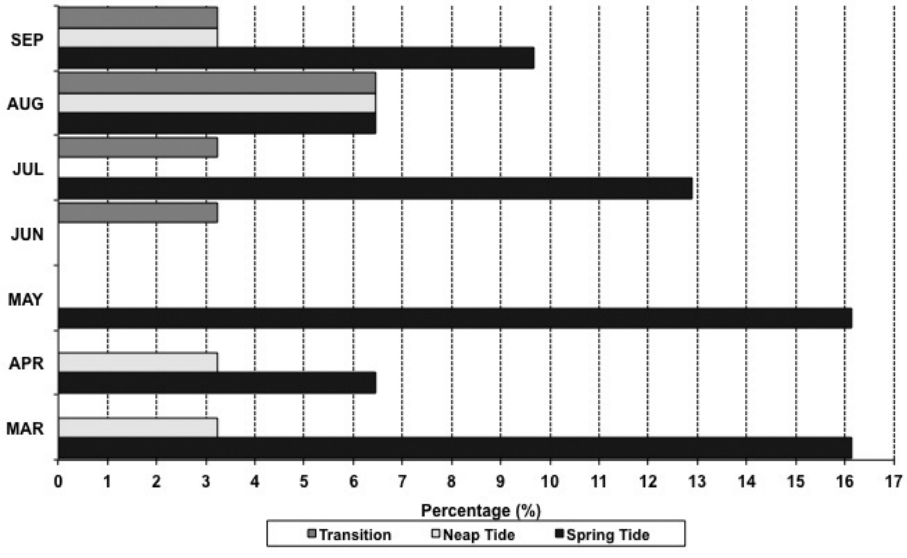

Figure 3 – Frequency of occurrence (in percentage) of tidal condition associated with erosion events during the period from 1965 to 2006 (Sources: *A Tarde* newspaper and National Observatory).

Conceptual model

Based on the criteria described in the methodology section for the construction of a conceptual model of erosion events on the Salvador coast, the process of coastal erosion (CE) was modeled by ranking the following terms from the most statistically significant to the least significant: tidal condition (T), synoptic systems (SS), waves (Wa) and interannual phenomena (IP), i.e.:

$$\mathrm{CE} = \mathrm{T} + \mathrm{SS} + \mathrm{Wa} + \mathrm{IP}.$$

Tidal condition (T)

Figure 3 shows that the maximum frequency of occurrence of spring tide erosion events was observed in March and May, with 16% of erosion events being associated with spring tides in each month. In July and September, this same tidal condition was associated with approximately 13% and 10% of the erosion events, respectively. In the months of April and August, only 6.5% of the erosion events occurred under the influence of a spring tide. Neap tides were the type of tide most frequently associated with erosion events during the month of August (approximately 6.5% of the events), while in the months of March, April and September, only approximately 3% of the events were associated with a neap tide. Erosion events occurring under the influence of transitional tides were concentrated in the months of August (approximately 6.5% of the events), and June, July and September (approximately 3%). According to Figure 3, spring tides

were the main driver of the erosion events occurring along the Salvador coastline from 1965-2006, when associated with storm surge, represented 68% of all erosion occurrences. In contrast, neap and tide transition periods were each associated with only 16% of the erosion events.

The high frequency of erosion events during the month of March can be attributed to the influence of large equinoctial tides, while the high frequency of erosion events during the months of May, July and September may be associated with other drivers because the monthly wind climatology provided by INMET shows the highest intensity values during that period. The maximum values of wind intensity observed in these months were possibly much more significant than tidal influences in contributing to the occurrence of erosion, especially considering the fact that an increased frequency of cold fronts along the coast of Bahia has also been observed during the winter season (Chaves, 1999; Andrade, 2005).

The parameters described below influence coastal erosion in Salvador through their direct and/or indirect relationship with atmospheric systems. The influence of these parameters are summarized as follows in the conceptual model:

i) S and SE winds operate in two different ways, piling up water directly against the shore or by Ekman transport. In the latter case, with the N-S orientation of the coast to the south of TSB, an increase in sea level would be propagated as a Kelvin wave and thus quickly reach the region. Such mechanisms were evidenced in TSB and the Bay of Camamú in studies by Cirano & Lessa (2007) and Amorim (2005), respectively. Janzen & Wong (2002) also described a similar type of coupling in Delaware Bay;

ii) a decrease in atmospheric pressure caused by the passage of synoptic systems associated with the inverted barometer effect, which results in increases in the mean coastal sea level and

iii) local or ocean waves originating from other regions, which may be accompanied by synoptic systems and could possibly act separately or simultaneously with coastal and ocean waves, thus contributing to the piling-up of water against the shore. In scenarios involving gravity waves, it is important to note the refraction of waves on the Salvador coast. This wave refraction promotes the convergence of wave energy at specific points on the coast, favoring sea level rise and the removal of sediment from the beach at these points and further exacerbating the process of coastal erosion.

Atmospheric conditions and synoptic patterns

In this section, the atmospheric conditions and synoptic patterns observed during the erosion events are described in terms of the behavior of the most significant parameters (wind, rainfall and MSLP).

Table 1 shows a comparison of mean u and v. Mean v during the erosion period was predominantly positive and lower (in absolute value) than mean u, with values of 3.0 m/s and -3.6 m/s for mean v and u, respectively. This mean wind field pattern relates to the predominant winds from the SE and S and is consistent with the proposed model, in which these winds cause the piling up of water against the shore. Additionally, the v component showed a greater degree of variation than the u component, which may represent a greater contribution of the meridional component as a result of Ekman transport. Ekman transport was quantified by analyzing the sign of the maximum values of wind v component during the EP of 27 events with prevailing winds from S to N, which accounted for 87% of the events in which Ekman transport predominated.

Monthly climatology data for mean wind speed in Salvador (Fig. 4) from INMET shows that the values of mean wind speed ranged between 1.8 m/s and 2.3 m/s throughout the year. As shown in Figure 4, the maximum values occurred between June and November, with the annual maximum occurring in July. This pattern indicates that high wind intensity from July to September may have contributed to the increased frequency of the erosion events observed during these months (Fig. 2).

Finally, the analysis of MSLP showed that mean MSLP for the erosion events was 1016 hPa (Table 1). The MSLP from the climatological time series (1968-1996) was approximately 1010 hPa from January to May and approximately 1015 hPa from October to December. In this data series, the highest values occurred from June to September, ranging from 1015 to 1020 hPa, which corresponds to a higher frequency of frontal systems reaching the east coast of the NEB. Based on a comparison of mean of the MSLP during erosion periods (1016 hPa) with the climatological MSLP cycle throughout the year, it appears that synoptic systems are intrinsically related to erosion events along the coast of Salvador.

To analyze the effects of atmospheric systems on coastal erosion processes, the erosion events were grouped according to the main synoptic features observed on the Salvador coastline during the EP. An event occurring on August 24-28, 1971 was excluded from this analysis because DHN had no corresponding synoptic map for that period and there was also no satellite imagery available. Therefore, 30 of the 31 events during the period from

Table 1 – Summary of the meteorological and oceanography drivers for the severe erosion events in Salvador during the period 1965-2006. Abbreviations for Cold Front (CF), High Pressure (HP) and Trough (TR) in the lower levels of atmospheric are indicated.

Number of events	Erosion events	Maximum Tidal Height (m)	Zonal and meridional wind (m/s)		Maximum and minimum wind (m/s)				Mean sea level pressure (hPa)	Synoptic systems	Inter-annual phenomena
			Mean ± Deviation (u)	Mean ± Deviation (v)	Zonal (u)		Meridional (v)				
1	07/17-20/67	2.1	–2 ± 1.5	5 ± 3.5	–4.7	0	9.5	–2.7	1016-1017	TR and HP	Neutral
2	06/03-07/69	2.2	–2 ± 2.0	–1 ± 3.0	–6.3	0.2	5.5	–5.2	1013	CF, HP, TR	El Niño
3	08/24-28/71	2.0	–3 ± 1.5	4 ± 0.0	–5.1	–0.6	6.2	2.9	1018	NO DATA	La Niña
4	06/30 to 07/03/74	2.1	–2 ± 2.0	8 ± 1.8	–6.0	2.2	11.0	5	1019-1020	TR and HP	La Niña
5	05/22-26/75	2.5	–1.5 ± –1.8	9 ± 1.7	–5.0	1.0	13.8	4.9	1017	TR and HP	La Niña
6	05/27-31/75	2.5	–3 ± 0.0	5 ± 1.4	–4.7	0.6	7.6	2.4	1015	TR and HP	La Niña
7	08/27-30/80	2.5	–4 ± 0.0	4 ± 3.0	–6.7	–1.0	9.8	–1	1019	CF, HP, TR	El Niño
8	04/04-07/81	2.7	–4 ± 1.0	2 ± 1.5	–5.7	–2.4	4.4	–0.7	1014	TR and HP	Neutral
9	03/15-19/84	2.8	–2 ± 1.8	3 ± 2.7	–5.5	1.5	9.5	–1	1011.5	CF, HP, TR	La Niña
10	08/01-04/85	2.4	–5 ± 1.8	5 ± 1.2	–8.4	–2.5	6.7	3.7	1020	TR and HP	La Niña
11	07/12-16/88	2.2	–3 ± 1.5	7 ± 2.5	–6.0	–0.2	12.5	3.8	1020-1022	CF, HP, TR	La Niña
12	07/31 to 08/03/88	2.5	–4 ± 1.5	5 ± 1.5	–7.3	–2.4	8.6	3.5	1019	TR and HP	La Niña
13	08/16-19/93	2.6	–4 ± 1.5	4 ± 1.5	–6.3	–1.3	6.8	0.0	1017-1018	TR and HP	El Niño
14	03/07-10/94	2.3	–2 ± 1.5	–1 ± 2.0	–5.1	0.3	2.5	–4.6	1011.5	CF, HP, TR	El Niño
15	07/08-12/94	2.4	–3 ± 2.0	2 ± 4.0	–8.5	0	9.6	–4	1019	CF, HP, TR	El Niño
16	04/15-18/95	2.6	–4 ± 1.6	3 ± 1.5	–7.7	–2.8	6.0	0.0	1012.5	TR and HP	El Niño
17	03/04-07/96	2.5	–5 ± 1.4	–1 ± 1.0	–8.2	–3.6	0.4	–3.4	1011	TR and HP	La Niña
18	04/18-21/96	2.4	–3 ± 1.5	4 ± 4.0	–5.6	–0.8	10.4	–2.4	1012	CF, HP, TR	La Niña
19	07/21-25/96	2.0	–4 ± 0.0	–6 ± 3.0	–6.4	–0.4	11.8	–1.0	1018	CF, HP, TR	La Niña
20	07/30 to 08/02/96	2.6	–4 ± 1.6	5 ± 1.5	–6.7	–2.2	7.4	2.1	1019	TR and HP	La Niña
21	09/10-13/96	2.3	–7 ± 1.8	2 ± 0.0	–10.7	–4.4	4.7	0.6	1018	TR and HP	La Niña
22	03/08-11/97	2.7	–3 ± 1.0	2 ± 1.2	–9.2	–3.1	4.2	0.5	1013	TR and HP	El Niño
23	03/27-30/99	2.4	–5 ± 2.1	0 ± 1.8	–8.2	–1.5	4.0	–3.0	1012.5	TR and HP	La Niña
24	05/13-16/99	2.7	–3 ± 1.5	5 ± 3.5	–5.2	–0.4	10.1	–1.0	1014	TR and HP	La Niña
25	09/26-29/99	2.5	–4 ± 1.5	3 ± 1.5	–6.2	–1.7	6.7	–1.7	1016	TR and HP	La Niña
26	03/21-24/01	2.4	–4.5 ± 1.5	1 ± 1.2	–7.5	–2.3	3.2	0.0	1013-1012.5	TR and HP	La Niña
27	05/21-25/01	2.5	–2.5 ± 2.0	4 ± 2.0	–6.5	1.1	6.7	1.0	1015	TR and HP	La Niña
28	09/16-19/01	2.7	–1.5 ± 2.0	3 ± 5.0	–6.5	–1	11.0	–5.0	1016	CF, HP, TR	La Niña
29	05/24-27/02	2.5	–1 ± 2.0	6 ± 1.5	–4.7	1.7	7.8	3.4	1016	CF, HP, TR	El Niño
30	09/21-24/05	1.9	–5 ± 2.0	0 ± 1.8	–7.2	–1.5	3.0	–2.8	1013-1015	CF, HP, TR	Neutral
31	09/05-10/06	2.8	–5 ± 2.0	4 ± 4.0	–8.5	–1.2	9.0	–3.7	1018	CF, HP, TR	El Niño
Mean	—	2.4	–3.6	3.0	–5.7	–0.2	7.3	–0.8	1016	—	—

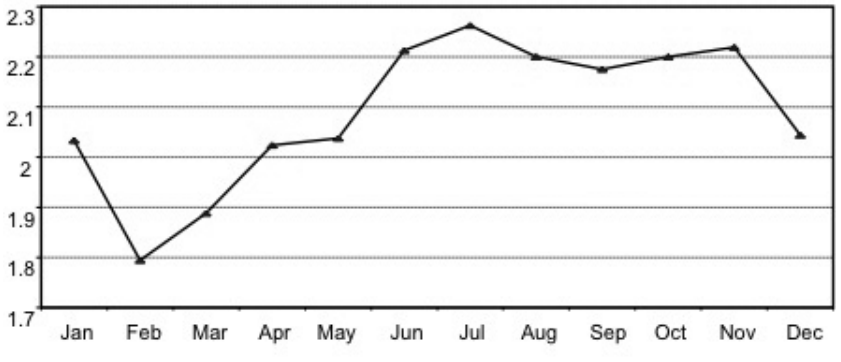

Figure 4 – Monthly mean climatology of the surface wind speed (m/s) in Salvador from 1975 to 1998 (Source: INMET).

1965-2006 were included in the analysis. Synoptic patterns related to erosion events along the Salvador coast were grouped into two types of scenarios, namely:

Scenario 1: in which the main synoptic characteristic was the simultaneous action of three large-scale systems (High Pressure (HP), Cold Front (CF) and Trough (TR)) in the lower levels of the atmosphere. There were two possible versions of this scenario:

(1A) No intersection of the CF with land during the EP (CF in the latitudinal range between 15°S and 20°S);

(1B) Intersection of the CF with the continent during the EP (in Salvador or nearby to the north or south), and;

Scenario 2: in which the main feature was the simultaneous action of two large-scale systems (HP and TR) in the lower levels of the atmosphere. There were two versions of this scenario:

(2A) No intersection of the CF with the continent during the EP (CF in the latitudinal range between 15°S and 40°S);

(2B) Intersection of the CF with the continent during EP (CF in the latitudinal range between 15°S and 25°S).

Table 2 – Total distribution of events for the synoptic scenarios 1A, 1B, 2A, and 2B.

Scenario	Number of events	Percentage
1A	6	20%
1B	6	20%
2A	9	30%
2B	9	30%

As shown in Table 2, 60% of the erosion events corresponded to Scenario 2, showing a mean synoptic pattern formed by coupling of the HP center and the TR at low levels, with the predominance of a SE wind along the Salvador shoreline on the days that the erosion events occurred. The remaining events (40%) occurred with a mean synoptic pattern in which the main configuration was a CF (Scenario 1). In these cases, the predominance of a surface wind in the S-SE direction could be observed, especially after the passage of the frontal system during the EP, which typically occurred on the day before erosion.

Scenario 1A (Fig. 5), which accounted for a total of 6 erosion events (20%), was characterized by a CF positioned in the latitudinal range between 15°S and 20°S, with a SE-NW orientation. In all cases, the CF intercepted this latitudinal range in the SW sector of its axis during the ED when it was positioned over the ocean. In events lasting more than one day (a total of 4 events), the CF shifted eastward over the ocean (typically on the second day of the EP), moving away from the continent and giving way to the HP coupled with a TR at low levels. The exception was one event in which the CF remained stationary during the erosion days and intercepted the 15°S latitude. In most events, the main axis of the TR was parallel to the east coast of the NEB, favoring upward movement of the surface winds, which were predominantly blowing from an E, SE and S direction. A notable feature in all of the events of this scenario type was the presence of the HP behind the CF, intersecting the continent and oscillating between the latitudes of the southern and southeastern regions of the country. Figure 5 shows an idealized schematic of Scenario 1A with the identified synoptic patterns.

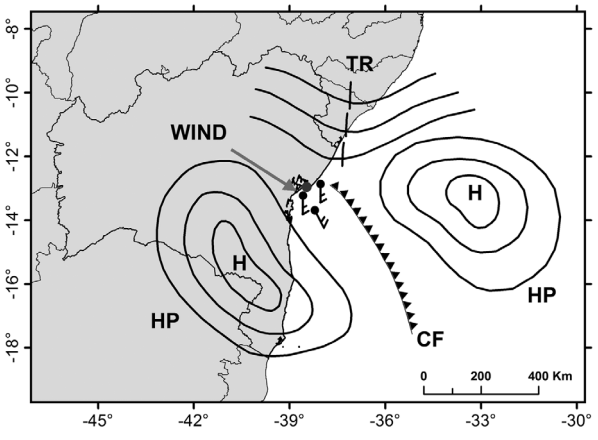

Figure 5 – Idealized schematic of the synoptic pattern observed in Salvador during the erosion events of Scenario 1A.

The wind u component had an E-W direction in almost all events corresponding to Scenario 1A, i.e., u component had negative intensities ranging from -8.5 to -1.5 m/s. The passage of the CF was confirmed by the change of direction in v component on the day before or on the ED, and the intensity of this component ranged from -5.2 to 12.5 m/s. On average, MSLP for this scenario ranged from between 1011.5 to 1022.0 hPa.

Scenario 1B (Fig. 6), which was characterized by a CF occurring in the latitudinal range between 15°S and 20°S with a SE-NW orientation on the day before the erosion event, was represented by six events or 20% of all events (Table 2). In these events, unlike with Scenario 1A, on the ED the CF advanced towards the north and intercepted land, in most cases reaching latitudes below 15°S. An important feature of this scenario was the weak activity of the TR, identified by the weak pressure gradient in some events. In other events in which the TR was more strongly formed, the main axis of the TR was aligned predominantly over the ocean, somewhat parallel to the east coast of the NEB, thereby contributing to the occurrence of SE winds, as

observed in two events. The surface synoptic maps showed that in 83% of the events, the wind was in a SE, S or SW direction, consistent with the combination of the synoptic systems operating in this scenario type (CF, HP and TR). The HP system always occurred behind the CF, centered in the ocean, and in all situations, the HP system intercepted the continent along its left boundary, oscillating between the latitudes of the southern and southeastern regions of the country.

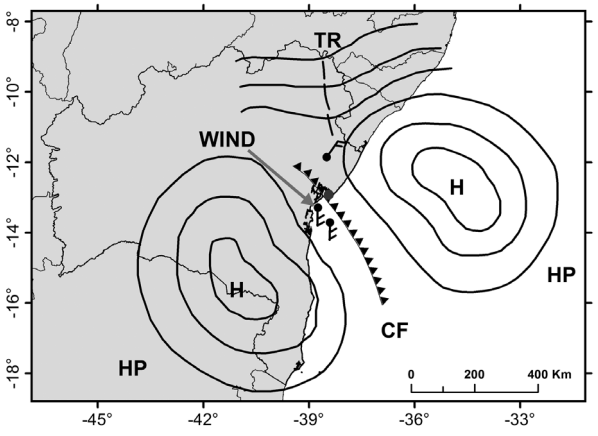

Figure 6 – Idealized schematic of the synoptic pattern observed in Salvador during the erosion events of Scenario 1B.

Spatial variations in the u wind component include extreme levels of intensity, ranging between -7.2 and 1.7 m/s. The u component was predominantly negative in 67% of the erosion events, except in two events, where this component occasionally oscillated and changed direction. The v wind component ranged between -5.0 and 11.8 m/s. In 83% of the events, this component changed direction or inverted its sign in the two days before the erosion event, thus marking the passage of the CF that always occurred when the wind was oriented in the E to S quadrant.

The pressure field varied between 1019 and 1011 hPa during all events for this scenario type. Based on the results of the analysis, it was possible to create an idealized synoptic pattern for this scenario in relation to the prevailing atmospheric circulation on the coast of Salvador during erosion events (Fig. 6).

On the day before the erosion and/or on the ED, the passage of frontal systems caused a conjunction of spring tides and the predominance of the S and SE meridional component in approximately 67% of the 12 erosion events corresponding to Scenario 1.

Scenario 2A (Fig. 7) accounted for 30% (Table 2) of the erosion events and was characterized by the left edge of the main axis of the TR positioned parallel to the eastern sector of the NEB between the latitudes of 0° to 20°S, thus favoring SE winds at the ocean-continent boundary. The HP system was always centered on the ocean between 15°S and 40°S, and its left boundary intercepted land in most events. Another striking feature of this scenario was that the wind direction oscillated between E and S in 89% of the events, with the direction of the wind being predominantly SE on the days prior to erosion and/or on the ED. Figure 7 shows an idealized schematic of this scenario for erosion events on the coast of Salvador.

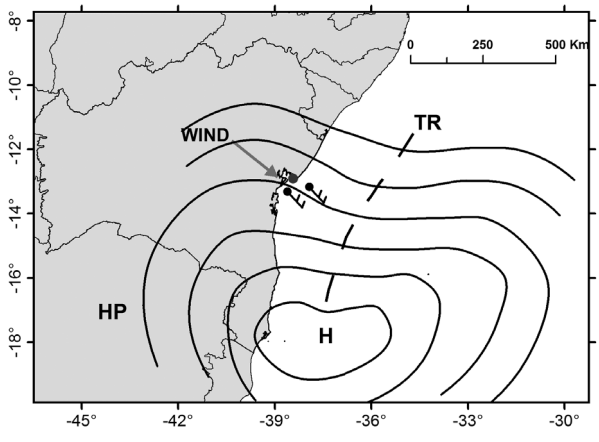

Figure 7 – Idealized schematic of the synoptic pattern observed in Salvador during the erosion events of Scenario 2A.

Extreme spatial variation in the wind u component occurred in Scenario 2A events, with intensities ranging between -9.2 and 1.0 m/s. In 67% of erosion events, this component was predominantly negative, except in three events, when the zonal wind component oscillated in direction, sometimes changing sign. The wind v component ranged from -3.0 to 13.8 m/s, and this component had a sign inversion in 44% of events. On average, the velocity of the wind u and v components ranged between -5 and -2 m/s and 0 to 5 m/s, respectively. Larger standard deviation values (up to 3.5 m/s) were observed for the meridional component, reflecting the high variability of this component, both in terms of intensity and direction, during the erosion events (Table 1). Sea level pressure varied on average between 1012.5 and 1019 hPa.

Scenario 2B (Fig. 8) also represented 30% of the erosion events (Table 2). The main characteristic of this scenario was the coupling of the synoptic systems HP and TR in the coastal region. The striking difference between Scenario 2B and Scenario 2A was the presence of a CF oscillating in the latitudinal range between 15°S and 25°S in 78% of Scenario 2B events, sometimes occurring over the ocean and sometimes intercepting land. It was also evident that wind direction oscillated in the SE quadrant in this scenario both on the day before and on the ED in 78% of the events. Figure 8 shows the synoptic pattern prevailing on the coast of Salvador during erosion events categorized as Scenario 2B.

In this final scenario, there was extreme spatial variation in the zonal wind component, with intensities ranging between −10.7 and 2.2 m/s, and this component was predominantly negative in 78% of the erosion events. In contrast, the meridional component ranged from −0.7 to 11.0 m/s. Mean u and v ranged between −7.0 and −2.0 m/s and −1.0 and 8.0 m/s, respectively (Table 1). The maximum standard deviation for both components was 2.0 m/s. Thus, it can be assumed that the wind components varied greatly in intensity. The MSLP field varied between 1011 and 1020 hPa for all events.

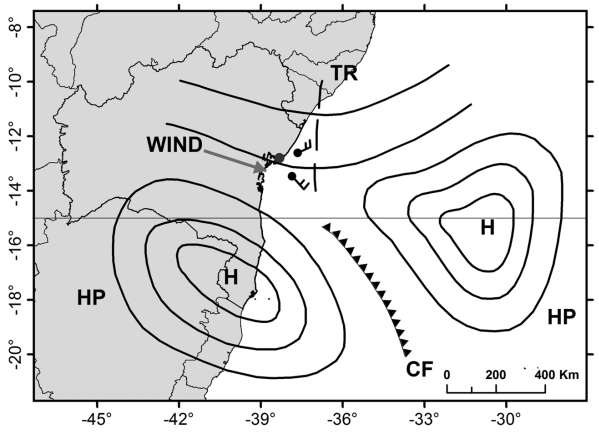

Figure 8 – Idealized schematic of the synoptic pattern observed in Salvador during the erosion events of Scenario 2B.

The higher frequency (60%) of erosion events categorized as Scenario 2 can be explained by the convection associated with the presence of the left boundary of the TR interacting at the ocean-continent boundary. This process favors the rapid development of vertical convection and sometimes the rapid dissipation of that convection. According to Freitas & Silva Dias (2004), this convection can be associated with the local circulation of sea breeze. The authors found, through a case study, a relationship between the propagation and intensity of sea breezes and certain large-scale systems for the metropolitan region of São Paulo. They found that the positioning of the high pressure zone was crucial for the increase and/or decrease in intensity of the sea breeze cell and its propagation. In an analysis of a time series of coastal winds, Franchito et al. (1998) observed a strong sea breeze near the coast of Cabo Frio, Rio de Janeiro when upwelling occurred and found that the interaction between the upwelling and the sea breeze can intensify physical processes involving the ocean-atmosphere interface. For example, Cavalcanti et al. (2006) showed that the interaction of an inverted trough, together with the action of the sea breezes, was responsible for an extreme rainfall event in Caraguatatuba, São Paulo.

Waves

As shown in the conceptual model, waves also play a key role in coastal erosion processes on the coast of Salvador. To evaluate the influence of waves, quarterly climatologies were generated for wave direction (Fig. 9), period (Fig. 10) and height (Fig. 11) in the study area.

Figure 9 shows the proportion of various mean wave front directions for the 12 sectors (Hogben & Lumb, 1967), corresponding to the monthly quarters MAM, JJA, SON and DJF. In MAM, wave direction ranged from 330° to 120°, with a predominance of waves in the ENE and E directions (25% and 20% of waves, respectively). During this quarter, wave periods of less than or equal to 5 s represented 58% of the total wave frequency (Fig. 10). The same E and NE wave directions predominated during JJA (approximately 35% and 25% of waves in the E and NE direction, respectively), but wave direction oscillated between 360° and 150°. The predominant wave period during this quarter was between 6 and 7 s (approximately 39% and 32% of waves, respectively), and wave periods were similar in the SON quarter. In both the SON and DJF quarters, wave direction was between 330° to 120°, with a relatively high occurrence of waves in the E, ENE, NNE and N directions. However, the proportion of waves in each direction differed between the two quarters. In SON, approximately 27% of waves were in the ENE direction, and 19% of waves were in the E, N or NNE directions. In DJF, waves in the N direction predominated (25%), followed by waves in the ENE (24%), NNE (21%) and E (17%) direction. Wave periods ranging between 8 and 9 s were more frequent in the JJA quarter (approximately 14% of waves), while periods longer than 9 s were rare.

Figure 11 shows that high sea waves with heights equal to or less than 1.5 m were predominant throughout the year with a maximum frequency in the DJF quarter accounting for approximately 70% of all waves. The waves with heights of 2 and 2.5 m occurred at maximum frequencies of approximately 27 and 13%, respectively, during the JJA quarter. Waves with heights exceeding 2 m were more frequent in the JJA quarter, with a frequency of approximately 27%. In this same quarter, waves with heights greater than or equal to 3 m occurred at a frequency of 7%. In the MAM, SON and DJF quarters, 2 m high waves accounted for 21%, 23% and 22% of all waves, respectively.

Based on the wave climatology data (Bittencourt et al., 2008), Figure 12 shows a refraction diagram of waves from the SE direction (135°) with a height and period sea wave of 2.0 m and 6.5 s, respectively. In this diagram, clusters of converging waves with heights greater than 2 m can be observed. These clusters coincide with the locations of the Atlantic coastal beaches of

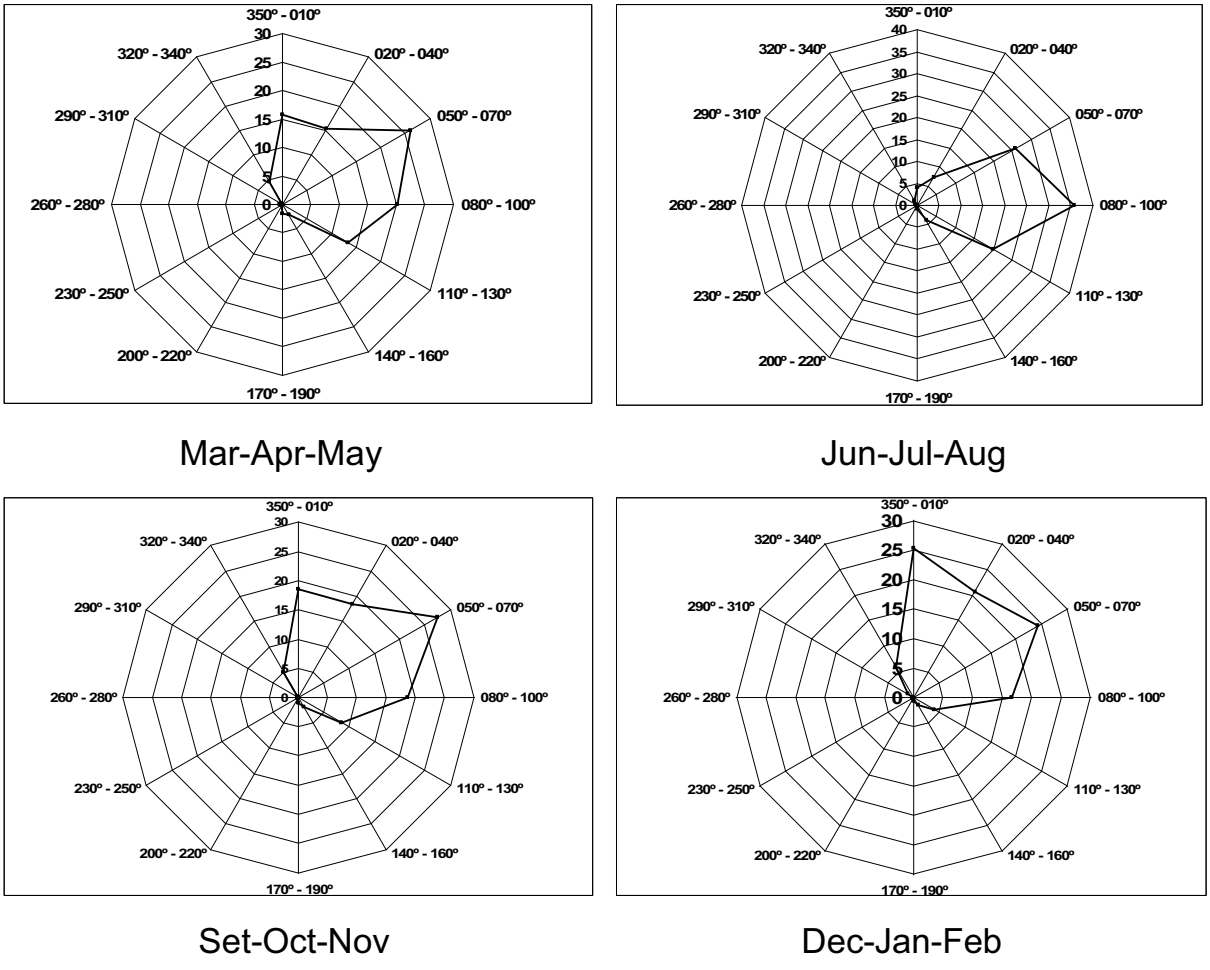

Figure 9 – Quarterly climatology of the wave direction (°) throughout the year for the coastal area of Salvador (adapted from Hogben & Lumb, 1967), represented by the percentage of occurrence in each direction.

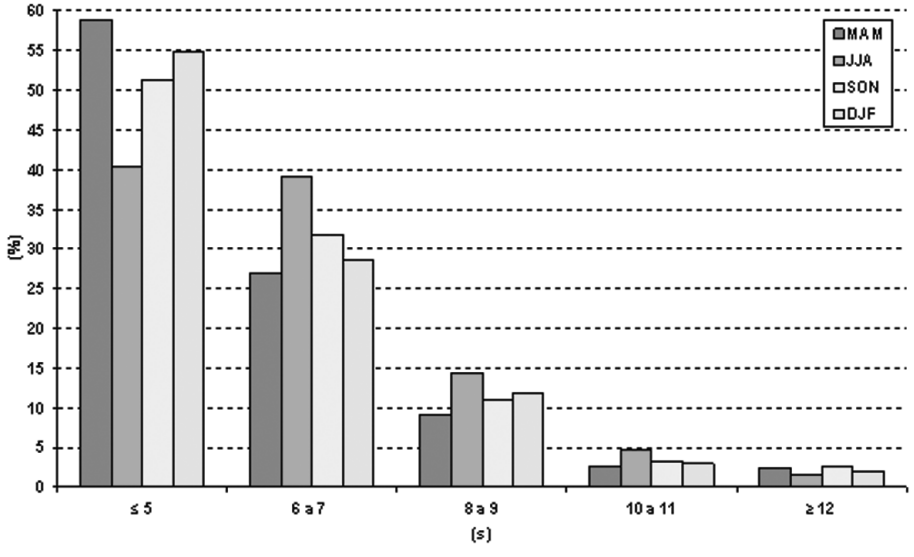

Figure 10 – Quarterly climatology of the wave period (s) throughout the year for the coastal area of Salvador (adapted from Hogben & Lumb, 1967), represented by the percentage of occurrence in each direction.

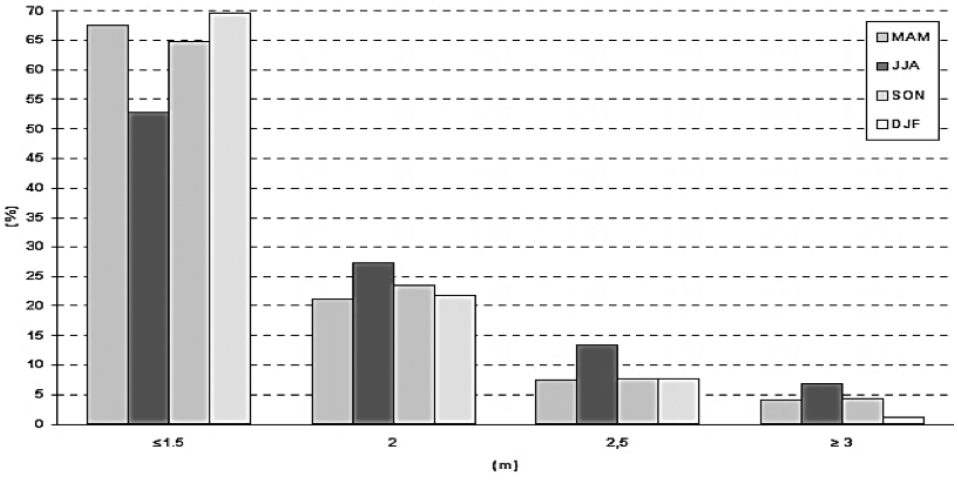

Figure 11 – Quarterly climatology of the significant wave height (m) throughout the year for the coastal area of Salvador (adapted from Hogben & Lumb, 1967), represented by the percentage of occurrence in each direction.

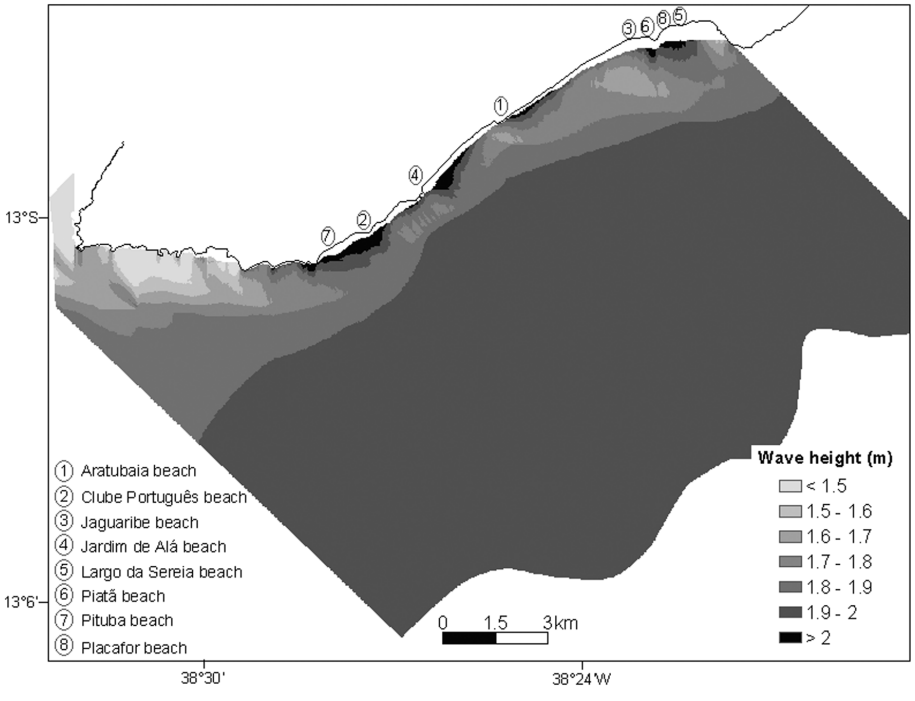

Figure 12 – Wave refraction diagram for the coastal area of Salvador to waves with 6.5 s period, 2.0 m height and SE direction. Extracted from Bittencourt et al. (2008).

Salvador where events of severe coastal erosion have historically occurred with the greatest frequency (Bittencourt et al., 2008). The importance of a SE wave direction in causing coastal erosion events on the Atlantic coast of Salvador has been noted in previous studies (Medeiros, 2005; Bittencourt et al., 2008). In the present study, the climatology for wave direction (Fig. 9) shows that the highest occurrence of waves with a direction in the ESE octant (20%) was in the JJA. This high frequency of ESE waves should be related to the high frequency of frontal systems during the same period (Kousky, 1979 and 1980; Chaves, 1999; Andrade, 2005). In addition, the highest frequency of high sea waves between 2 and 2.5 m in height was attained in JJA (Fig. 11), which were likely to have grown larger in the clusters of converging waves on the Salvador coast. This led to increased

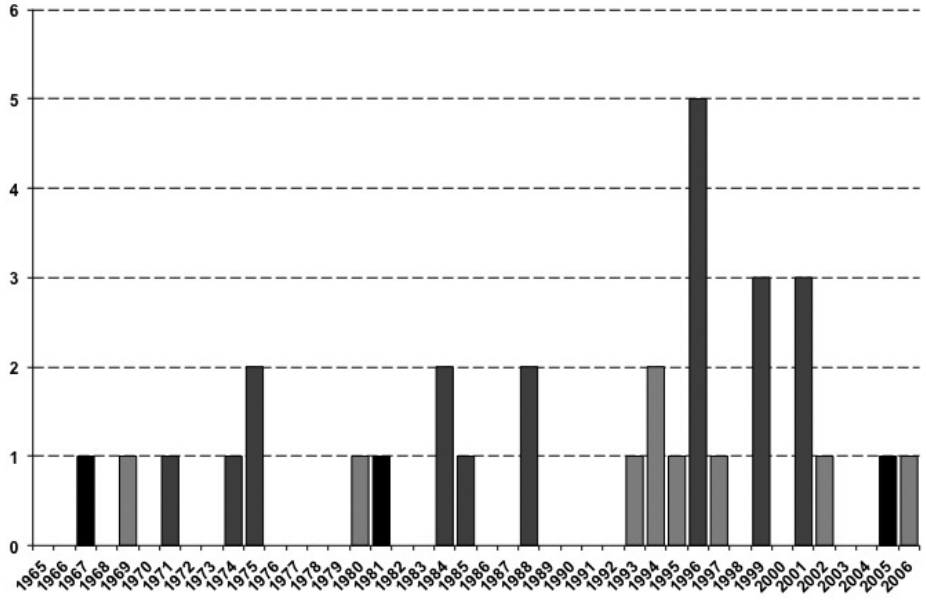

Figure 13 – Annual frequency of occurrence of erosion events in Salvador coastline and SST pattern in the Central Equatorial Pacific for years with occurrence of El Niño (light gray), La Niña (dark gray) and neutral (black) (CPTEC).

erosion, as described by Bittencourt et al. (2008). Following JJA, the second highest frequency of waves in the ESE octant, about 14% of all waves, was observed in MAM. This may have favored, in addition to the equinoctial tides, the high occurrence of coastal erosion along the Salvador coastline (Fig. 2).

Interannual phenomena

The parameters were analyzed by order of importance, and the last parameter to be analyzed was interannual phenomena (IP). The results showed that El Niño and La Niña also influence the frequency of coastal erosion on the Salvador coastline. It is known that ENSO alters the normal pattern of atmospheric circulation in both its warm and cold phases, leading to variation in wind regimes and rainfall in tropical and mid-latitudinal regions, with impacts at the regional and global scale. In the NEB, droughts occur in the northern part in El Niño years during the climatological rainy season from February to May. The southern and western parts of this region are not significantly affected by IP (Kousky et al., 1984; Aceituno, 1988). However, the arrival of cold fronts over the NEB occurs more frequently during La Niña years, mainly along the coasts of Bahia, Sergipe and Alagoas (Ropelewski & Halpert, 1987; Lima 1991; Moura et al., 2000). The authors cited here have also observed that there is a greater likelihood of above average rainfall in the semi-arid northeast region when La Niña occurs simultaneously with above average SST in the tropical South Atlantic and below average SST in the tropical North Atlantic.

Given the importance of ENSO for the climate of the NEB, we examined the influence of ENSO on erosion events on the coast of Salvador. The events were grouped by year of occurrence and correlated with the index that defines the intensity of the ENSO phenomenon. This index was obtained from CPTEC/INPE and is a function of wind intensity based on the pattern and magnitude of SST anomalies in the tropical Pacific. Figure 13 shows that the highest frequency of erosion events (60% of events) occurred under the influence of La Niña events. In contrast, only 30% of the erosion events occurred under the influence of El Niño. Additionally, in neutral years when anomalies were close to zero in the Pacific, three erosion events (10%) occurred. The maximum annual frequency of erosion events (5 events per year) occurred in 1996, followed by the years 1975 and 1988 (2 events per year) and 1999 and 2001 (3 events per year). All of these years coincided with La Niña events. For erosion events associated with El Niño, the maximum annual frequency was two events per year, which occurred in 1994.

Based on these analyses, it appears that the El Niño and La Niña phenomena have the indirect effect of increasing and decreasing the frequency of coastal erosion, respectively, on the coast of Salvador. In addition, during the erosion events associated with La Niña years, the meridional wind component was more intense than in El Niño years, with a mean meridional wind component of 3.5 and 2.5 m/s for La Niña and El Niño years, respectively. This pattern of more intense meridional winds during La Niña years was also identified by Piola et al. (2000).

Table 3 verifies the association of ENSO with the synoptic pattern and tidal conditions observed during the erosion events. The table shows that among the Scenario 1A and 1B events, five events (42%) occurred during La Niña and six (50%) occurred during El Niño. Only one event occurred in a neutral year. With respect to tides, erosion events most often occurred during spring tides during both La Niña and El Niño years. These results show that the ENSO phenomenon has a less clear and less direct effect on the occurrence of erosion events of the Scenario 1 type. For events in the Scenario 2A and 2B categories, the influence of La Niña was stronger. La Niña was associated with 13 erosion events (approximately 72% of events of these scenario types), with 10 events (approximately 55%) occurring simultaneously with a spring tide. The remaining 28% of the erosion events occurred under the influence of El Niño (16.7%) and in a neutral year (11.1%).

Table 3 – Erosion events organized according to La Niña (L), El Niño (E), and neutral conditions (NT) and with tidal conditions – spring (S), transition (T) and neap tide (N).

	Erosion events (number)	SST			
		L	E	NT	
Scenario 1A and 1B	03/15-19/84 (9)	X			S
	07/12-16/88 (11)	X			
	07/08-12/94 (15)		X		
	09/16-19/01 (28)	X			
	05/24-27/02 (29)		X		
	09/05-10/06 (31)		X		
	08/27-30/80 (7)		X		T
	03/07-10/94 (14)		X		
	04/18-21/96 (18)	X			
	06/03-07/69 (2)		X		N
	07/21-25/96 (19)	X			
	09/21-24/05 (30)			X	
Scenario 2A and 2B	07/17-20/67 (1)			X	S
	06/30 to 07/03/74 (4)	X			
	05/22-26/75 (5)	X			
	05/27-31/75 (6)	X			
	04/04-07/81 (8)			X	
	08/16-19/93 (13)		X		
	04/15-18/95 (16)		X		
	03/04-07/96 (17)	X			
	07/30 to 08/02/96 (20)	X			
	09/10-13/96 (21)	X			
	03/08-11/97 (22)		X		
	03/27-30/99 (23)	X			
	05/13-16/99 (24)	X			
	03/21-24/01 (26)	X			
	05/21-25/01 (27)	X			
	08/01-04/85 (10)	X			T
	09/26-29/99 (25)	X			
	07/31 to 08/03/88 (12)	X			N
	Total	18	9	3	

For the events that occurred in association with neap and transitional tides during El Niño and during normal years (June 3-6, 1969; August 27-30, 1980; March 7-10, 1994 and September 21-24, 2005) (Table 3), it appears that there was another external driver of erosion, or the other factors in the conceptual model (i.e., cold fronts, waves and Ekman transport) had a strong enough influence to overlap the effect of tides, resulting in coastal erosion on the Salvador shoreline.

Case studies

This study aimed to investigate and understand the atmospheric and oceanographic conditions that affect coastal erosion events on the Salvador coastline. To that end, the major synoptic and oceanographic driving forces affecting two specific erosion events are discussed here. The two events correspond to two types of synoptic patterns, i.e., Scenarios 1 and 2. The two events occurred on March 15-19, 1984 and May 22-26, 1975 and corresponded to Scenarios 1A and 2A, respectively. These two events were chosen for the case study analysis due to the relatively high level of material damage caused by these events on the coast of Salvador, which was determined using information obtained from local newspapers.

Erosion event of March 15-19, 1984 (Scenario 1A)

The predicted maximum tide heights during the erosion period of this event were 2.8 m, corresponding to a spring tide that occurred between March 17 and 18 and 2.7 m, which occurred on March 16-19. The predicted maximum tide (2.8 m) exceeded the mean tide height for all erosion events during the study period by 40 cm.

Atmospheric parameters for the March 15-19, 1984 erosion event are shown in Figures 14 to 18.

As shown in Figure 14a, the zonal wind had an initial value of −3.0 m/s and oscillated before reaching its minimum intensity the erosion period (approximately 1.5 m/s at 12 UTC on the 17th). Maximum intensity occurred at 12 UTC on the 19th, with a value of approximately −5.5 m/s. A change of direction was observed twice, first from 06 UTC to 12 UTC and then from 12 UTC to 18 UTC on the 16th. Even on days when there was no change in wind direction, a strong oscillation in zonal wind intensity was observed. The amplitude of this oscillation was approximately 4.0 m/s.

For the meridional wind component, Figure 14b shows an initial value of 4.1 m/s and a maximum value of approximately 9.4 m/s (at 12 UTC on the 16th). The lowest value (approximately −1.0 m/s) was recorded on the 19th at 12 UTC. This wind component had a S direction during most of the EP and reversed

direction (from S to N) only after 06 UTC on the 19th. The component amplitude was 10.4 m/s.

The mean and standard deviation of the zonal wind component were −2.5 m/s and 1.8 m/s, respectively, and the mean and standard deviation of the meridional wind component were 4.0 m/s and 3.0 m/s, respectively. Thus, the meridional component showed the highest mean and standard deviation values, which reflects the behavior of this component as described in the overall analysis of Scenario 1A presented above.

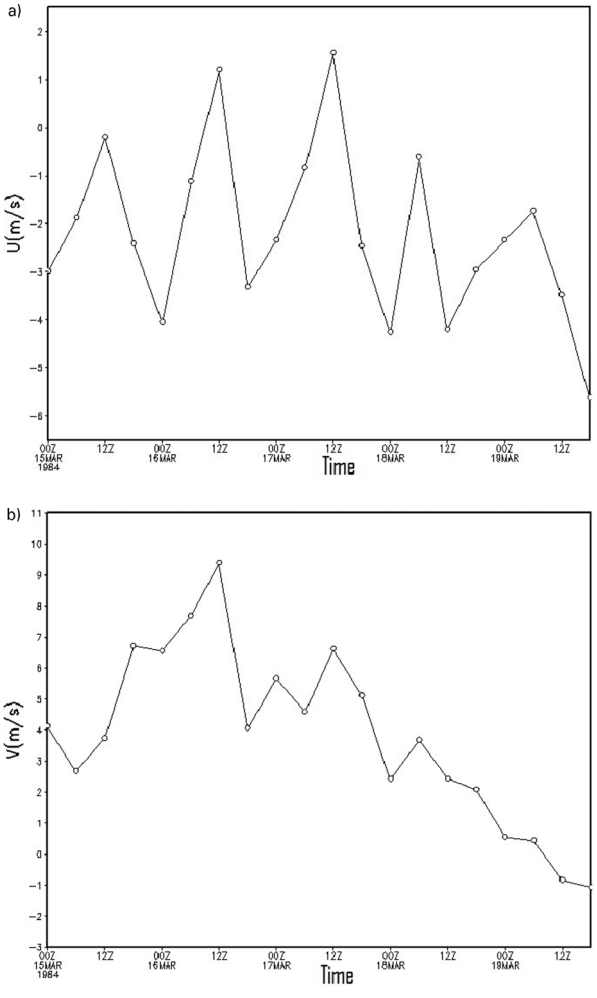

Figure 14 – Mean variation of the (a) zonal and (b) meridional wind components at 10 m, from the NCEP reanalysis, between 39.5°W, 14.0°S and 37.0°W, 12.5°S during the erosion event of March 15-19, 1984.

The MSLP field (Fig. 15) shows the typical pattern for Scenario 1A events, with a trough along the coast of the NEB and a cold front located over the ocean.

The analysis using the surface synoptic maps from the DHN/Brazilian Navy Hydrographic Center (Centro de Hidrografia da Marinha – CHM/DHN) (Fig. 16) showed the presence of a CF close to Salvador on March 15th (Fig. 16a), with its cloud band oriented in the SE-NW direction over the ocean. The presence of a HP center (1020 hPa) behind the front resulted in SE winds with an approximate intensity of 7.7 m/s on the coast of Salvador. On March 16th (Fig. 16b), there was an intensification and coupling of the HP center (1024 hPa) with a TR in the low levels of the atmosphere. The axis of this system was over the ocean but had an orientation parallel to the east coast of NEB. Due to this configuration, winds reached a maximum intensity of 15.3 m/s and were primarily oriented in a SE direction close to the coast of Salvador. In contrast, the CF on that day shifted completely over the ocean. On March 17th (Fig. 16c), the CF retreated towards land, and the convective band exhibited a SE-NW direction near the latitude of Salvador, favoring S winds with an intensity of approximately 5.1 m/s to the south of Salvador. On March 18th (Fig. 16d), the CF retained the same characteristics as observed on the previous day. Only the wind direction changed, shifting to the SE, with an intensity of 2.6 m/s to the south of Salvador. On the last day of the EP (March 19th) (Fig. 16e), the CF dissipated and gave way to a HP system (1016 hPa) that coupled with a low-intensity TR, favoring weak winds of about 2.6 m/s with a SE direction in Salvador.

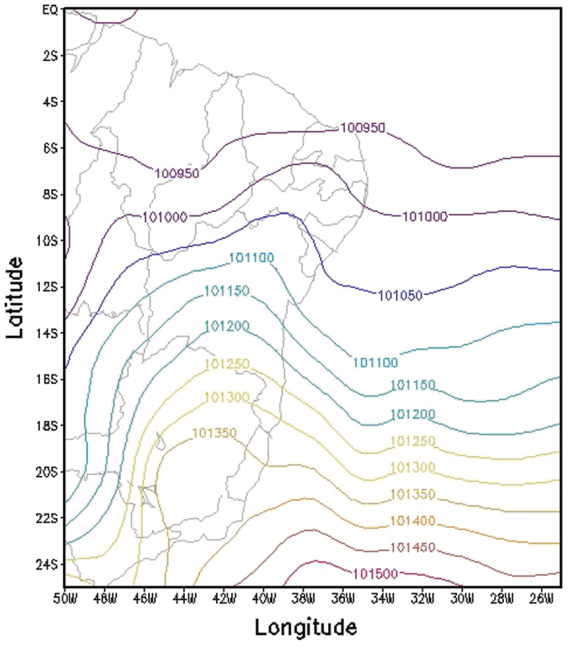

Figure 15 – Mean sea level pressure (Pa) during the erosion period (03/15 to 03/19/84) (NCEP).

These results show that when the direction of the meridional wind is reversed from N to S, the standard deviation and maximum intensity associated with the large-scale pattern of the cold front may explain the occurrence of large high sea waves, which further increase in the clusters identified by Medeiros

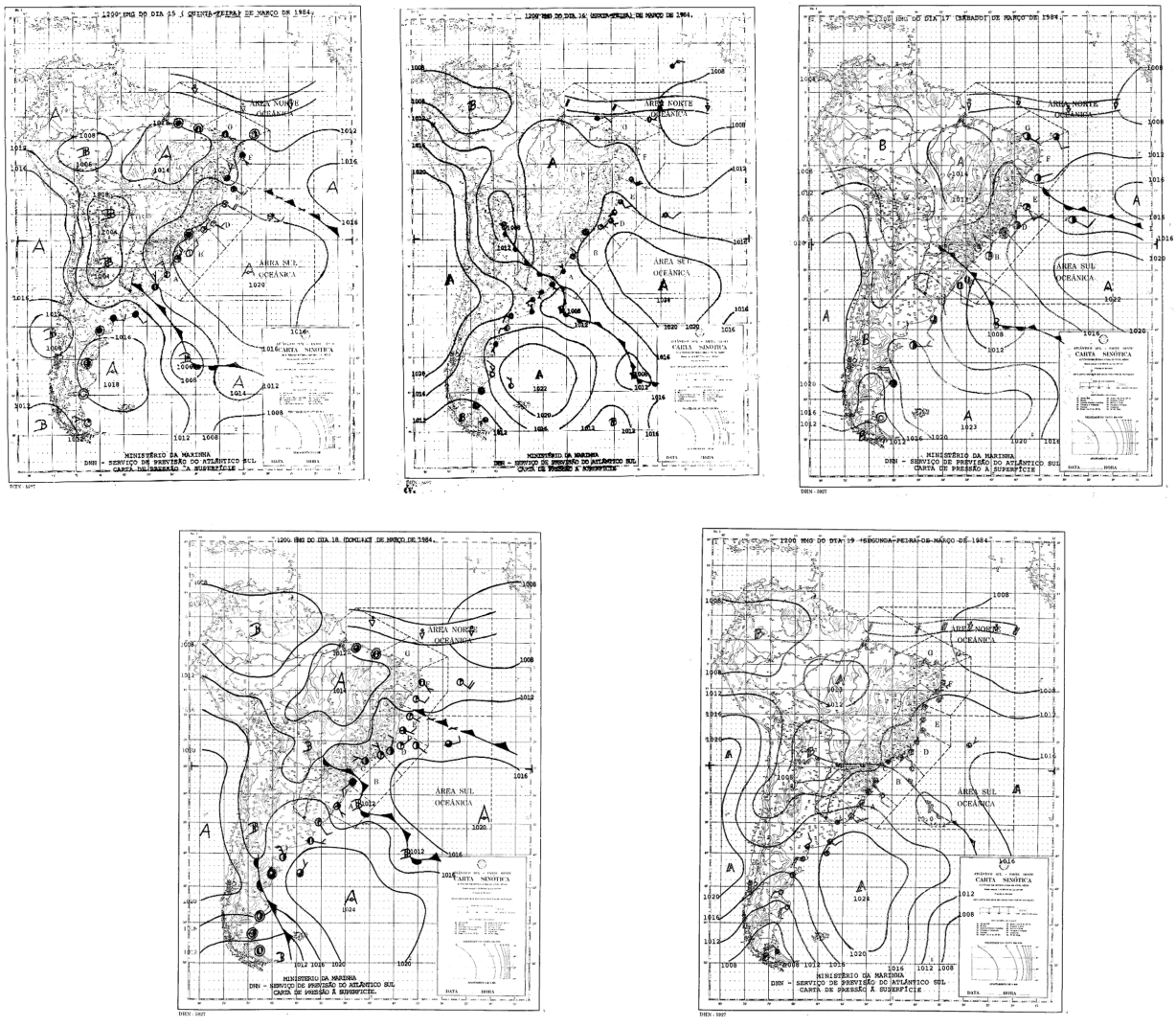

Figure 16 – Surface synoptic maps at 12 UTC for the days: (a) Upper left panel – 03/15, two days before the erosion; (b) Upper center panel – 03/16, one day before the erosion; (c) Upper right panel – 03/17 and (d) Lower left panel – 03/18, erosion days; and (e) Lower right panel – 03/19, one day after the erosion (Source: CHM/DHN).

(2005) and Bittencourt et al. (2008) along the Salvador coast. It was also observed that, due to the behavior of the meridional wind during the EP, Ekman transport was oriented toward the shore, leading to increased sea levels and the amplification of the erosion event.

Table 4 and Figure 17 were produced with the ERA-40 reanalysis and show the maximum high sea values for the significant wave height (1.8 m) and wave period (8.0 s) that occurred on March 16th at 12 UTC. It is likely that the waves were generated locally by the passage of the cold front, as they had a wave period of less than 12 s.

Finally, it is worth noting that a weak La Niña was also present during this erosion event and may have contributed to the increased frequency of cold fronts on the coast of Bahia.

Table 4 – Maximum observed values for the sea wave height and period before the erosion day (03/16/84) and in the erosion days (03/17/84 and 03/18/84), with the respectively occurrence hours (Source: ERA-40 from ECMWF).

Days	Maximum sea wave height (m)	Maximum period (s)	Time (UTC)
03/16/84 (BE)	1.8	8	12
03/17/84 (ED)	1.6	8	12 and 18
03/18/84 (ED)	1.6	8	00

Erosion event of May 22-26, 1975 (Scenario 2A)

For this event, the predicted maximum tide heights for the erosion period were 2.5 m, corresponding to a spring tide between May 23 and 25, and 2.4 on May 22 and 26. The maximum expected tide (2.5 m) exceeded the mean tide for all erosion events over the

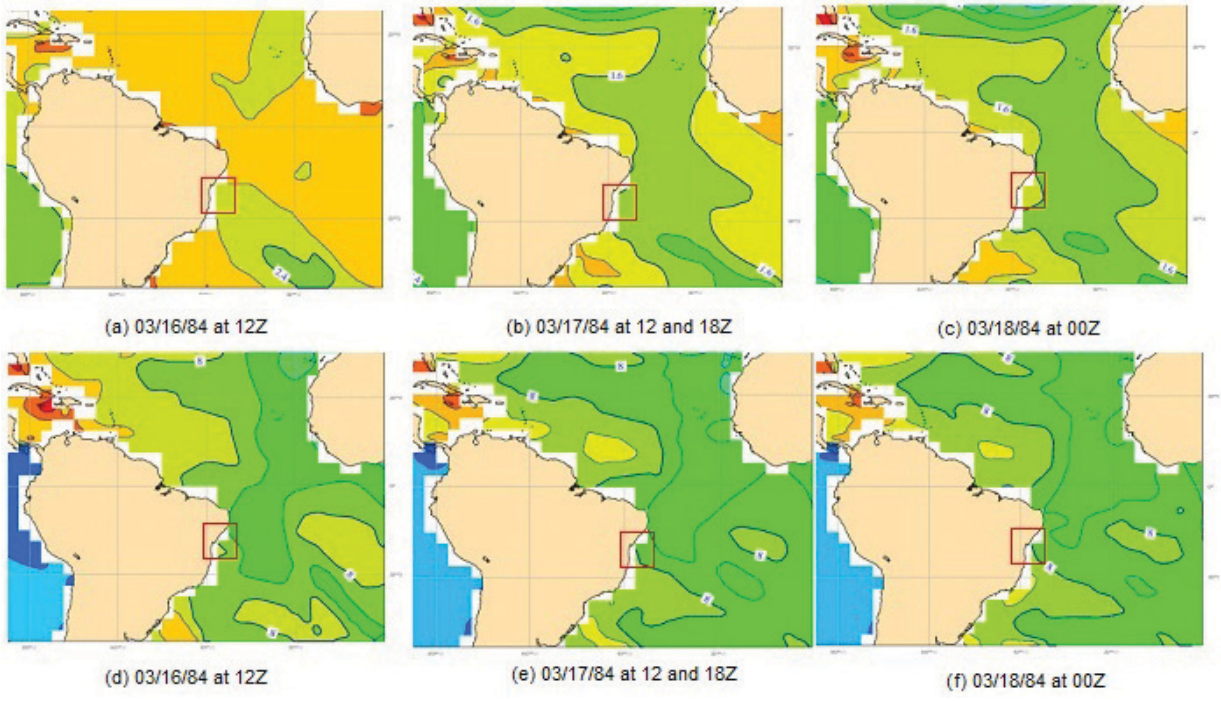

Figure 17 – Significant wave height (a), (b), (c) and wave period (d), (e) and (f) for the day before the erosion (03/16) and in the erosion days (03/17 and 03/18), respectively. Contour intervals in the figures are equal to 0.6 m (a); 0.4 m (b), (c); and 1 s (d), (e), (f); respectively (Source: ERA-40).

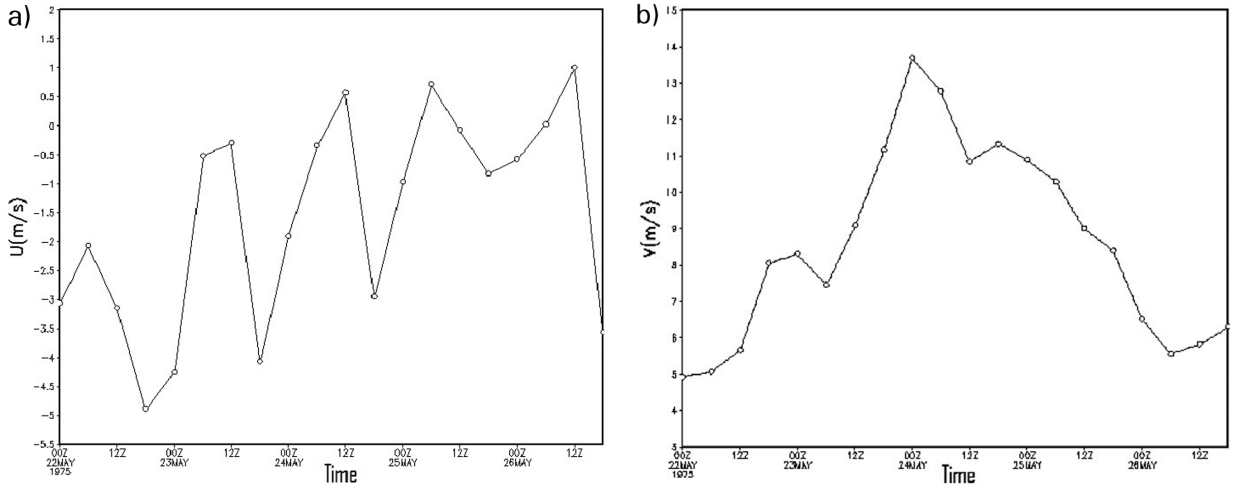

Figure 18 – Mean variation of the (a) zonal and (b) meridional wind components at 10 m, from the NCEP reanalysis, between 39.5°W, 14.0°S and 37.0°W, 12.5°S during the erosion event of March 22 to 26, 1975.

study period by 10 cm.

Figure 18a shows that the zonal wind component had an initial value of approximately −3.0 m/s at 00 UTC on May 22nd. The maximum and minimum values were −4.9 m/s at 18 UTC on the May 22nd and 1.0 m/s at 12 UTC on May 26th. It is important to note that this component changed direction six times between May 24th and 26th, and its amplitude during this period was −3.9 m/s. The maximum value of the meridional component (Fig. 18b) was approximately 14.7 m/s on May 24th at 00 UTC, and the minimum value was 4.9 m/s at 00 UTC on May 22nd. The oscillation amplitude of this component was approximately 9.8 m/s.

The mean and standard deviation values for the zonal component during the EP were −1.5 m/s and 1.8 m/s, respectively. The mean value for the meridional component was 8.0 m/s, and the standard deviation was approximately 2.7 m/s.

In the typical pattern of Scenario 2A, a high pressure system dominates Bahia, Minas Gerais and the surrounding region (Fig. 19), and a trough with a meridional structure is present over the ocean. The MSLP field favors average E-SE winds in a vast oceanic region at tropical latitudes and triggers waves towards the coast of Bahia.

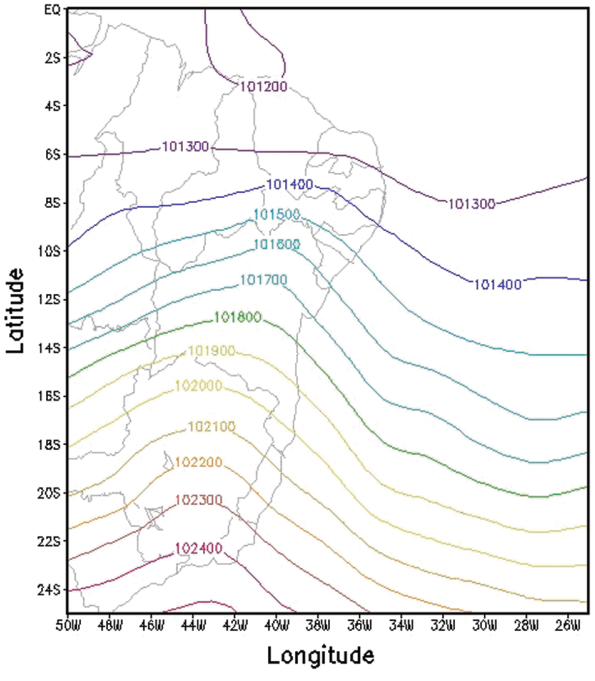

Figure 19 – Mean sea level pressure (Pa) during the erosion period (05/22 to 05/26/75) (NCEP).

The overnight evolution of the MSLP field and winds can be observed in the CHM/DHN surface synoptic maps presented in Figure 20. On May 22nd (Fig. 20a), a TR was present in the low levels of the atmosphere with its main axis centered on the east coast between the states of Pernambuco and Rio de Janeiro. This system was found to be associated with a HP center (1028 hPa) located over the ocean near the southeast coast of Brazil that dominated much of the central-eastern, southern and northeastern regions. The weather conditions associated with the circulation were unstable, with S-SE winds located over the coast of Bahia. On May 23rd (Fig. 20b), the TR over the coastline dissipated and the prevailing winds near the coast of Salvador became E-oriented with an intensity of approximately 7.7 m/s. On May 24th (Fig. 20c) and 25th (Fig. 20d), a TR formed over the ocean, and an intensification of the pressure gradient was observed, confirmed by a maximum wind intensity of approximately 10.2 m/s in the SE and S directions. On the last day of the EP (Fig. 20e), the TR weakened. Wind intensity decreased, but the wind direction remained SE.

As shown in the Scenario 1A case study, the predominance of winds in the S or SE direction explains the occurrence of large high sea waves that are later heightened at convergence cluster identified by Medeiros (2005) and Bittencourt et al. (2008) along the coast of Bahia. The standard deviation of the meridional component was approximately 2.7 m/s, which indicates atypical behavior of the meridional component when compared with the mean wind flow during this period. This behavior can be attributed to the coupling of the HP and TR synoptic systems, as evidenced in the synoptic maps. Similarly to the case study for Scenario 1A, in this case study, the meridional wind component during the EP promoted Ekman transport directed towards the coast, contributing to increased sea levels and intensification of the erosion event.

For the oceanographic parameters, Table 5 and Figure 21 show that the maximum value of significant wave height (2.5 m) and wave period (9.0 s) at high sea occurred on May 25th at 06 UTC. These data indicate that the waves originated locally because they have a period of less than 12 s. Thus, the waves may also be related to the coupling of the HP and TR systems.

Table 5 – Maximum observed values for the sea wave height and period before the erosion day (05/23/75) and in the erosion days (05/24/75 and 05/25/75), with the respectively occurrence hours (Source: ERA-40).

Days	Maximum sea wave height (m)	Maximum period (s)	Time (UTC)
05/23/75 (BE)	2.5	8.0	18
05/24/75 (ED)	2.0	8.8	12
05/25/75 (ED)	2.5	9.0	00

Finally, it is worth mentioning that a strong La Niña was active during this erosion event. The La Niña phenomenon may have influenced oceanic-atmospheric conditions in the South Atlantic basin and favored the intensification of high frequency synoptic systems, resulting in surface winds. During the erosion period, the predicted maximum tide height was less pronounced (2.5 m), which suggests that other factors in the conceptual model, including synoptic systems and waves, acted together with an astronomical tide to cause a rise in sea levels and intensify erosion near Salvador.

CONCLUSION

The results of this study show that the penetration of cold fronts and high pressure centers, coupled with troughs in the low

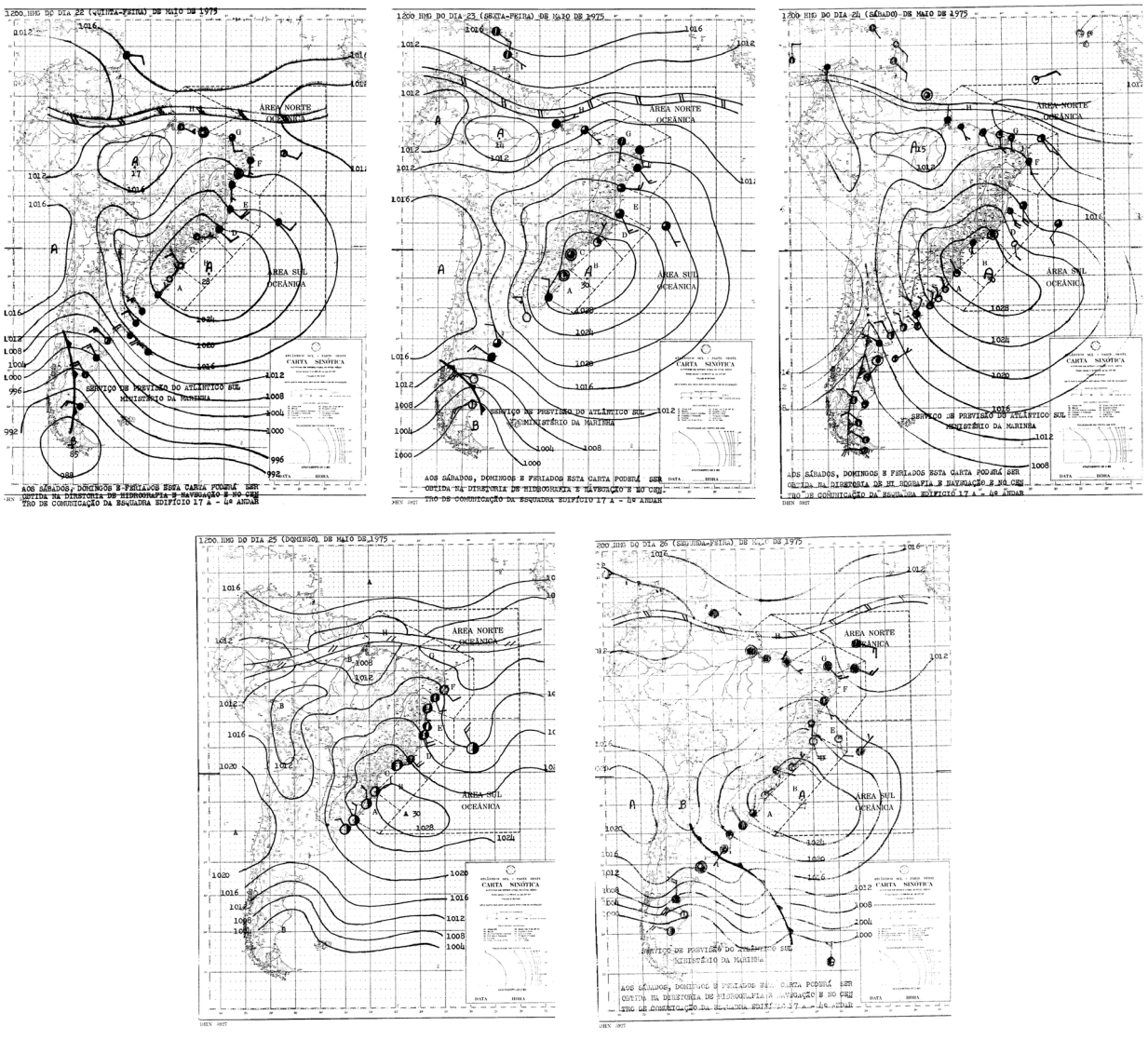

Figure 20 – Surface synoptic maps at 12 UTC for the days: (a) Upper left panel – 05/22, two days before the erosion; (b) Upper center panel – 05/23, one day before the erosion; (c) Upper right panel – 05/24 and (d) Lower left panel – 05/25, erosion days; and (e) Lower right panel – 05/26, one day after the erosion (Source: CHM/DHN).

levels of the atmosphere, are key to explaining the development of severe erosional processes in wave convergence clusters, especially when combined with the occurrence of a spring tide. This last factor is a necessary condition for the occurrence of erosion events in Salvador. The atmospheric and oceanic circulation patterns produced in the four scenarios described in the conceptual model in this study induced Ekman transport, S and SE winds and wave height. Together with spring tides, these factors drove the severity of erosion events that caused a relatively big economic loss.

In most of the erosion events examined in this study, there was a predominance of winds from the S and SE, which replaced trade winds from the E through the passage of frontal systems. As a result, coastal circulation associated with Ekman transport caused water to be pushed towards the shore, and this sea level height is a direct function of wind speed. The accumulation of water raised the tide, causing the water to advance beyond the coastline and reach the highest parts of the beach, removing sediment from the beach through the action of the waves.

Two specific events of severe coastal erosion on the coast of Salvador (corresponding to Scenarios 1A and 2A from the conceptual model) were used as case studies to validate the proposed conceptual model and examine in-depth the atmospheric and oceanographic patterns that were active during the events.

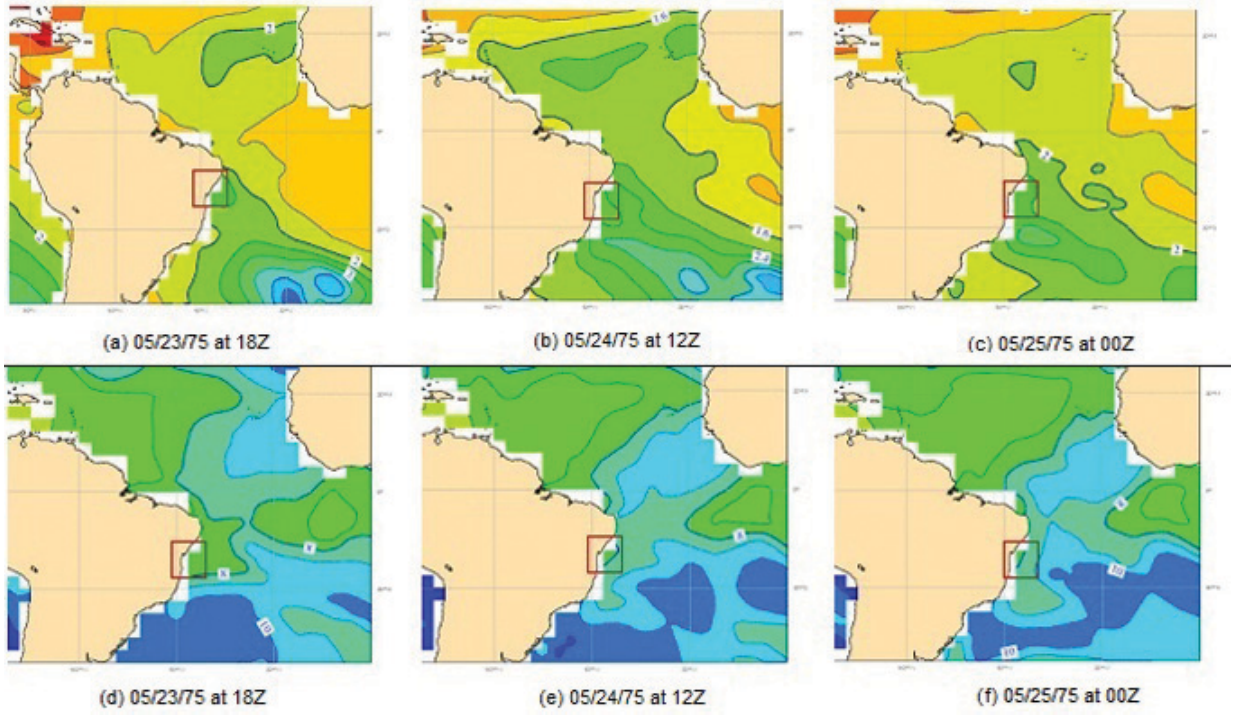

Figure 21 – Significant wave height (a), (b), (c) and wave period (d), (e) and (f) for the day before the erosion (05/23) and in the erosion days (05/24 and 05/25), respectively. Contour intervals in the figures are equal to 0.5 m (a), (c); 0.4 m (b); and 1 s (d), (e), (f), respectively (Source: ERA-40).

The results of the case studies suggest that waves were caused by the interaction between local and remote phenomena. Waves moved towards the coast after being refracted and rose at the wave convergence clusters previously proposed by Medeiros (2005) and Bittencourt et al. (2008). In both erosion events, the meridional wind component during the erosion period resulted in Ekman transport directed toward the coast, which contributed to a rise in sea level.

Furthermore, with the prospect of rising sea levels as a result of global warming from increased concentrations of greenhouse gases in the atmosphere, it is expected that erosion events at the wave convergence clusters identified in this study will intensify.

ACKNOWLEDGMENTS

The authors kindly thank MSc. Felipe Moraes Santos for designing Figures 1, 5, 6, 7 and 8 of this manuscript. Mauro Cirano and Abilio C.S.P. Bittencourt were supported by CNPq research grants.

REFERENCES

ACEITUNO P. 1988. On the Functioning of the Southern Oscillation in the South America Sector. Part I: Surface Climate. Monthly Weather Review, 116: 505-524.

BITTENCOURT ACSP, DOMINGUEZ JML, MARTIN L & SILVA IR. 2000. Patterns of sediment dispersion coastwise the State of Bahia – Brazil. Anais Academia Brasileira de Ciências, 72(2): 271–287.

BITTENCOURT ACSP, DOMINGUEZ JML, MARTIN L & SILVA IR. 2005. Longshore transport on the northeastern Brazilian coast and implications to the location of large scale accumulative and erosive zones: An overview. Mar. Geol., 219(4): 219–234.

BITTENCOURT ACSP, MEDEIROS KOP, DOMINGUEZ JML, GUIMARÃES JK & DUTRA FRLS. 2008. Severe Coastal Erosion Hotspots in the City of Salvador, Bahia, Brazil. Shore & Beach, 76(1): 8–14.

CHAVES RR. 1999. Variabilidade da precipitação na região sul do Nordeste e sua associação com padrões atmosféricos. Master dissertation, São José dos Campos (SP), Brazil, INPE, 159 pp.

CIRANO M & LESSA GC. 2007. Oceanographic characteristics of Baía de Todos os Santos, Brazil. Brazilian Journal of Geophysics, 25(4): 363–387.

DOMINGUEZ JML & BITTENCOURT ACSP. 1996. Regional Assessment of Long-Term Trends of Coastal Erosion in Northeastern Brazil. Anais Academia Brasileira de Ciências, 68(3): 355–371.

GRIMM AM. 2003. The El Nino impact on the summer monsoon in Brazil: Regional processes *versus* remote. J. Climate, 16(2): 263–280.

HASLETT SK. 2000. Coastal Systems. Routledge introductions to environment series. Routledge, London, 218 pp.

HOGBEN N & LUMB FE. 1967. Ocean Wave Statistics. National Physical Laboratory. Ministry of Technology, London, 263 pp.

INMET. Instituto Nacional de Meteorologia. 2010. Ministério da Agricultura e Reforma Agrária, Brasil. Normais Climatológicas (1961-1999), Versão Revista e Ampliada. Brasília. 465 pp.

KOMAR PD. 1998. Beach processes and sedimentation. New Jersey: Prentice-Hall, 2 ed. 544 pp.

KOUSKY VE. 1979. Frontal influences on Northeast Brazil. Mon. Weather Rev., 107: 1140–1153.

KOUSKY VE. 1980. Diurnal rainfall variation in northeast Brazil. Mon. Weather Rev., 108(4): 488–498.

KOUSKY VE & CHU PS. 1978. Fluctuations in annual rainfall in northeast Brazil. J. Meteorol. Soc. Japan, 56(5): 457–465.

KOUSKY VE, KAYANO MT & CAVALCANTI IFA. 1984. A review of the Southern Oscillation: oceanic-atmospheric circulation changes and related rainfall anomalies. Tellus, 36A: 490–504.

LIMA MC. 1991. Variabilidade da precipitação no litoral leste da Região Nordeste do Brasil. Master's Thesis in Meteorology. Instituto Nacional de Pesquisas Espaciais. São José dos Campos, 222 pp.

MEDEIROS KOP. 2005. Relação entre episódios de erosão severa na costa atlântica de Salvador com fenômenos meteorológicos, marés e zonas de convergência de ondas: subsídio para o gerenciamento costeiro. Salvador-Bahia, Honours Thesis in Geology. Universidade Federal da Bahia, 36 pp.

MURTY TS. 1988. List of major natural disasters, 1960-1987. Nat. Hazards, 1(3): 303–304.

NEVES SM. 2003. Erosão Costeira no Estado da Paraíba. Doctoral Dissertation. Instituto de Geociências da Universidade Federal da Bahia, 152 pp.

NEVES CF & MUEHE D. 1995. Potential Impacts of Sea-level Rise on the Metropolitan region of Recife, Brazil. J. Coast. Res., Special Issue 14: 116–131.

PARISE CK, CALLIARI LJ & KRUSCHE N. 2009. Extreme storm surges in the south of Brazil: atmospheric conditions and shore erosion. Braz. J. Oceanogr., 57(3): 175–188.

PIOLA AR, CAMPOS EJD, MÖLLER OO, CHARO M & MARTINEZ C. 2000. Subtropical Shelf Front off eastern South America. J. Geophys. Res., 99(C3): 655–678.

PIVEL MAG, SPERANSKI N & CALLIARI LJ. 2002. A erosão praial na costa Atlântica Uruguaia. Pesquisas em Geociências, 28(2): 447–457.

TESSLER MG & GOYA SC. 2005. Processos Costeiros Condicionantes do Litoral Brasileiro. Revista do Departamento de Geografia, 17: 11–23.

WANG CZ. 2002. Atlantic climate variability and its associated atmospheric circulation cells. J. Climate, 15(13): 1516–1536.

WANG CZ, LEE SK & MECHOSO CR. 2010. Interhemispheric Influence of the Atlantic Warm Pool on the Southeastern Pacific. J. Climate, 23(2): 404–418.

Recebido em 29 outubro, 2012 / Aceito em 11 outubro, 2013
Received on October 29, 2012 / Accepted on October 11, 2013

NOTES ABOUT THE AUTHORS

Flávia Regina Lacerda Suassuna Dutra has a bachelor degree in meteorology and a MSc degree in Coastal Geology at Universidade Federal da Bahia (UFBA), with focus on the influence of cold fronts in the coastal erosion of Salvador-Bahia-Brazil. Currently, is a Ph.D. student in Physical Geography at IGC – UFMG (Universidade Federal de Minas Gerais, Belo Horizonte-Brazil), finishing the thesis phase. The theme of her study provides the relation between climate and leptospirosis transmission in Minas Gerais state, this study is focused on environmental analysis. Currently, is funded by a CNPq scholarship.

Mauro Cirano is graduated in Oceanography from FURG (1991), has a MSc in Physical Oceanography from IOUSP (1995) and a Ph.D. in Physical Oceanography from the University of New South Wales (UNSW), Sydney, Australia (2000). Since 2004 has a permanent position at the Universidade Federal da Bahia (UFBA) and is currently an Associate Professor. Areas of research interest include the study of circulation processes in coastal and oceanic regions, both based on the analysis of oceanographic data, and through numerical modeling of the circulation. Since 2006 coordinates the regional modelling efforts of REMO. Also is a member of the Coastal Ocean and Shelf Seas Task Team (COSS-TT), linked to GODAE OceanView.

Abilio Carlos da Silva Pinto Bittencourt has a bachelor degree in Geology from Universidade Federal da Bahia (UFBA) in 1965 and a MSc in Geology from UFBA in 1972. Currently, is a professor at UFBA and a researcher at the National Council for Scientific and Technology Development (CNPq). Has experience in Geosciences with an emphasis on Geological Oceanography. Areas of expertise include: Coastal Evolution, Beach Morphodynamics, Coastal Processes, Refraction of Waves, Numerical Modeling of Coastal Drift and Potential Economic Damage Associated with Coastal Erosion.

Clemente Augusto Souza Tanajura is a mechanical-nuclear engineer with a Ph.D. in Meteorology by the University of Maryland, College Park, USA. Worked as a associate researcher at the Laboratório Nacional de Computação Científica (LNCC) during 18 years. Currently, is a Professor at the Universidade Federal da Bahia (UFBA). Was the technical-scientific coordinator of the Oceanographic Modeling and Observation Network (REMO) from December, 2008 to March, 2013 and

is member of the GODAE OceanView Science Team. Works with data assimilation, oceanic and atmospheric numerical modeling, short-term oceanic and atmospheric predictability, and climate studies.

Mateus de Oliveira Lima is an oceanographer and currently a MSc student in Physical Oceanography at the Geophysical Post-Graduate Program of the Universidade Federal da Bahia (UFBA). Is a team member of the MOVAR (Monitoring the upper ocean transport variability in the western South Atlantic) project. Currently, is working with comparisons of oceanic numerical models at the AX97 high density XBT line.